Journal of Zhejiang University-SCIENCE A (Applied Physics & Engineering)
ISSN 1673-565X (Print); ISSN 1862-1775 (Online)
www.zju.edu.cn/jzus; www.springerlink.com
E-mail: jzus@zju.edu.cn

Characteristics of strong winds at the Runyang Suspension Bridge based on field tests from 2005 to 2008*

Hao WANG†[1,2], Ai-qun LI[1,2], Chang-ke JIAO[1,2], Xing-ping LI[1,2]

([1]*MOE Key Laboratory of Concrete and Prestressed Concrete Structure, Nanjing 210096, China*)

([2]*College of Civil Engineering, Southeast University, Nanjing 210096, China*)

†E-mail: wanghao1980@seu.edu.cn

Received Oct. 6, 2009; Revision accepted Feb. 26, 2010; Crosschecked June 8, 2010

Abstract: Field measurement of strong wind characteristics is of great significance for the development of bridge wind engineering. Located in east China, the Runyang Suspension Bridge (RSB) with a main span of 1490 m is the longest bridge in China and the third longest in the world. During the last four years, the RSB has suffered from typhoons and strong northern winds on more than ten occasions. To determine the strong wind characteristics of the RSB, wind measurement data obtained from field tests during strong winds and data from the wind environment monitoring subsystem of the structural health monitoring system (SHMS) of the RSB were combined to analyze the wind speed and direction, variation in wind speed with height, turbulence intensity, turbulence integral length, wind friction speed and the power spectrum. Comparative studies on the characteristics of these different strong winds were carried out based on the current wind-resistant design specification for highway bridges. Results showed that some regularity in wind characteristics can be found in these different typhoons passing through the RSB. The difference between a strong northern wind and a typhoon is relatively clear, and in summer the typhoon is the dominant wind load acting on the RSB. In addition, there were some differences between the measured strong wind characteristics and the values suggested by the specification, especially in respect to turbulence intensity and turbulence integral length. Results provide measurement data for establishing a strong wind characteristic database for the RSB and for determining the strong wind characteristic parameter values of this coastal area in east China.

Key words: Suspension bridge, Strong wind, Wind characteristic, Field test, Structural health monitoring system (SHMS)
doi:10.1631/jzus.A0900601 **Document code:** A **CLC number:** U448.25

1 Introduction

Long-span bridges, tall buildings and other large structures above ground or sea level are usually sensitive to strong wind force (Davenport, 1962; Naito, 1988; Geurts *et al.*, 1996; Simiu and Scanlan, 1996). When these structures are close to coastal areas, wind is one of the most important loading factors for structural design (Choi, 1978; Geurts *et al.*, 1996). However, the response of structures when subjected to dynamic wind force is very complicated. Therefore, the refinement of our understanding of dynamic wind force and wind-induced structural response has become one of the most important issues in wind engineering research.

To calculate accurately the effect of wind on the structures, the characteristics of the wind acting on the structures must first be simulated precisely. The main characteristics include the mean wind characteristics and the turbulence wind characteristics, which form the basis of a 3D wind field simulation. The most effective method for determining the regional wind characteristics is to conduct extensive wind tests, and then analyze the data using statistical methods. Therefore, the experimental study of strong wind characteristics is of great value to the develop-

* Project supported by the National Natural Science Foundation of China (Nos. 50725828, 50908046, and 50978056), the National Science & Technology Pillar Program (No. 2006BAJ03B05), and the PhD Program Foundation of MOE (No. 200802861012), China

ment of wind engineering (Panofsky and Dutton, 1984; Vickery and Twisdale, 1995; Shiau and Chen, 2001; Ge and Xiang, 2004).

Since the 1970s, much progress in wind climate study has been achieved and in some countries databases containing information on aspects of wind characteristics have been established, such as the Sparks database of the USA (Sparks *et al.*, 1992), the Kato and Ohukuma database of Japan (Kato *et al.*, 1992), and the Froya database of Norway (Andersen and Lovseth, 1995). However, most of the databases are for meteorological applications. With the rapid development of structural health monitoring and sensor techniques in recent years, more and more wind data are being recorded all over the world (Vickery and Twisdale, 1995; Holmes, 2001; Rigato *et al.*, 2001; Miyata *et al.*, 2002; Siringoringo and Fujino, 2008; Tieleman, 2008; Hui *et al.*, 2009). In China, some wind measurement studies in civil engineering have also been conducted in recent years (Xu *et al.*, 2000; Pang *et al.*, 2002; Chen *et al.*, 2002; Li *et al.*, 2004; Xu and Zhu, 2005; Law *et al.*, 2006; Wang *et al.*, 2009). However, because the monitored strong wind data is far from sufficient, many wind characteristic parameters in China have to be estimated using research results from other countries, which is unreasonable as the wind characteristics are likely to be affected by geography. Therefore, it is especially significant and necessary to carry out field tests on the strong wind characteristics in Chinese mainland.

Meteorological studies show that the strong wind load acting on the Runyang Suspension Bridge (RSB) includes mainly the typhoons occurring in summer and the northern winds in winter. During the last four years, the RSB has suffered from several typhoons and strong northern winds, including the typhoons Matsa in August, 2005, Khanun in September, 2005, Saomai in August, 2006, Wipha in September, 2007, Kalmaegi and Fung-Wong in July, 2008. In some cases, the center of the typhoon passed through the RSB while in other cases the RSB was affected only by disturbances around the edge of the typhoon. Thus, the influence of each typhoon on the RSB is related not only to its wind speed, but also to its passing course. As for the strong northern winds which can be measured in winter every year, they are not as strong as the typhoons in general, but some may continue for many days, so special attention should also be paid to them.

In general, the wind data from the current wind-resistant design specification for highway bridges (Xiang, 2004) is used when no field measurements are available. Based on the data recorded from 657 wind measurement stations in China from 1961 to 1995, the specification was issued by the Ministry of Communications of China on Dec. 8, 2004. The contents of the specification include the basic wind speed, the design standard wind speed, the wind speed variation with altitude, the gust factor, the turbulence intensity, the turbulence integral length, the turbulence power spectrum density, the requirements for wind tunnel tests and wind-induced vibration control, etc. Moreover, the specification makes use of the information from the corresponding specifications of Europe, England BS5400, America, Japan, and Denmark.

In this study, to determine the strong wind characteristics, data from both the structural health monitoring system (SHMS) and the field tests were applied to conduct a comparative study of typhoon and strong northern wind characteristics at the site of the RSB. The research results were also compared with the current specification, to provide not only measurements for wind resistance safety assessment of the RSB, but also a reference for wind resistance design of other structures in this coastal area of eastern China.

2 Research background

As a national key engineering project, the Runyang Yangtze River Bridge which connects Zhenjiang city with Yangzhou city is composed of two long span bridges: the RSB located on the south side and the Runyang Cabled-stayed Bridge (RCB) on the north side of the Yangtze River. The RSB is a hinged and simply supported steel-box-girder bridge with a main single span of 1490 m and two side spans, each 470 m long (Fig. 1). It is the longest suspension bridge in China and the third longest in the world (Wang *et al.*, 2009) (The RSB will soon rank second in China with the opening of the Xihoumen Suspension Bridge with a main span of 1650 m).

For such an important bridge, it is essential to

conduct research on the surrounding wind to evaluate the effects on structural safety caused by extreme wind force. Therefore, a meteorological study was carried out by the Jiangsu Province Meteorology Research Institute in June, 2000. The study noted that the RSB is located in the northern region of the sub-tropical zone, with obvious subtropical monsoon climate characteristics. The cold and dry northern wind from the mainland is the main strong wind in winter, and in summer the typhoon dominates. The climate of the RSB is complex and there are many adverse weather events including typhoons, storms, and thunderstorms.

To monitor and assess the condition of the RSB during the building and operating period (Wang *et al.*, 2009), especially under the influence of storms, the Structural Health Monitoring Institute of Southeast University, China took charge of designing the SHMS of the Runyang Yangtze River Bridge. Fig. 2 shows the sensor layout in the SHMS.

To obtain wind measurement data and provide a reliable basis for evaluation of the wind resistance of the RSB, two anemometers were installed in the SHMS, one on the top of the south tower and the other in the middle of the main span (Fig. 2). In addition, some 3D Sonic anemometers were installed on the RSB as a supplement during the strong winds.

3 Anemometers and measurement locations

Two kinds of anemometers were installed in the field wind test of the RSB: the WA15 anemometer from the Vaisala Company (USA) and the 1590-PK-020 3D Sonic anemometer from the Gill Instruments Limited (Japan). Two WA15 anemometers were used in the SHMS of the RSB (Fig. 3a), and three 1590-PK-020 3D Sonic anemometers were installed only during strong winds (Fig. 3b).

One of the WA15 anemometers was deployed on

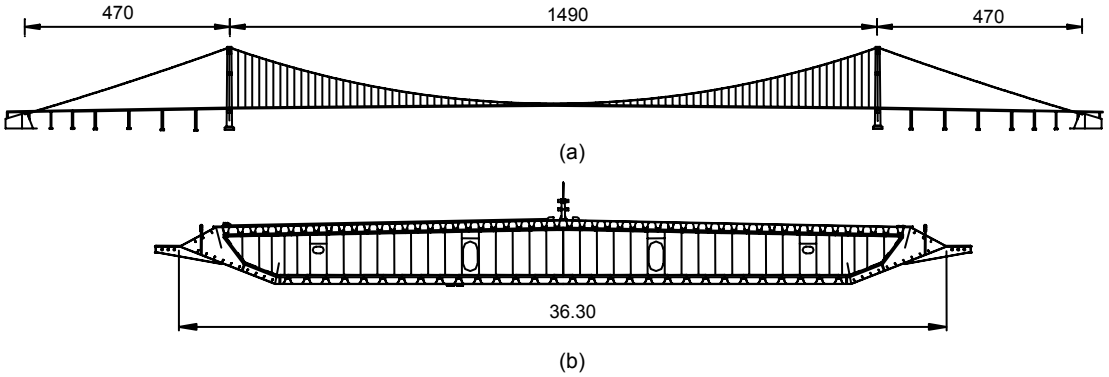

Fig. 1 Configuration of the RSB. (a) Elevation; (b) Cross-section of the steel box girder (unit: m)

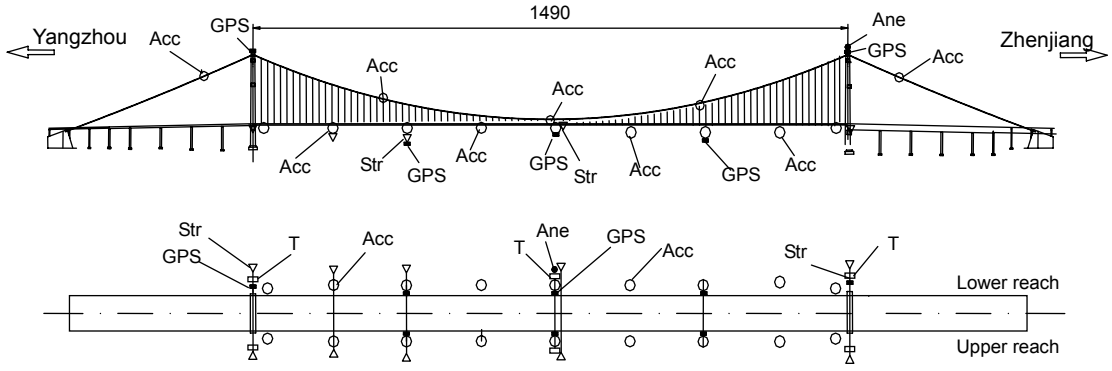

Acc: accelerometer (85); Str: stress conge (72); Ane: anemometer (2); T: temperature sensor (28); GPS: GPS receiver (8)

Fig. 2 Layout of sensor system of RSB (unit: m)

(a) (b)

Fig. 3 WA15 anemometer (a); 1590-PK-020 anemometer (b)

the top of the south tower (downstream) 218.905 m above ground and the other in the middle of the main span (upstream) 69.300 m above the ground. The anemometers were installed to the north, with the angle of the wind direction defined by 0° corresponding to the north. By the convention that positive rotation goes clockwise, east is 90°, and so on. Long-term successful applications in meteorological studies have shown that the WA15 anemoscope can work under all kinds of bad weather and accurately acquire the wind speed and direction.

The SHMS provides only average or maximum wind speed and direction data. It does not collect continuous time history wind speed and direction data when the frequency is greater than 1 Hz. Because of this limitation, in this study, three 1590-PK-020 3D Sonic anemometers were used in the field test during strong winds. The 1590-PK-020 anemometer with its light weight and small volume is especially well suited for working in the rain. The maximum sampling frequency can reach 100 Hz. Because of these features, the 1590-PK-020 anemometer is used widely in the wind testing of engineering structures. As these three anemometers can be installed in any location on the RSB depending on the purpose of the measurement, the turbulence integral length and spatial correlation of strong wind can be measured.

4 Analysis of measured strong wind characteristics

Wind characteristics are usually decomposed into the mean and turbulence wind characteristics when conducting wind engineering research. The mean wind characteristics contain the mean wind speed and direction, the wind speed variation with altitude, etc. The turbulence wind characteristics contain the turbulence intensity, the integral length, the power spectrum density, etc. During the last four years, the SHMS of the RSB has recorded typhoons and strong northern winds on more than ten occasions. Based on their wind speed and central course, only four typhoons were selected as typical examples in this study: typhoon Matsa in August, 2005, Khanun in September, 2005, Wipha in September, 2007 and Fung-Wong in July, 2008. Because of the regularity of the strong northern wind characteristics, only the data measurements recorded in March, 2007 were considered. All of these strong winds were analyzed to obtain comparative mean and turbulence wind characteristics. Note that all of the wind data were collected from the middle of the main span except for the data for typhoon Wipha, which were from the top of the south tower.

As the wind characteristics, duration and route of each typhoon differed greatly, the duration of each analysis period was different: typhoon Matsa from 00:00 on Aug. 5 to 06:00 on Aug. 6, 2005, typhoon Khanun from 19:15 on Sept. 11 to 17:15 on Sept. 12, 2005, typhoon Wipha from 06:00 on Sept. 19 to 04:00 on Sept. 20, 2007, typhoon Fung-Wong from 00:00 to 14:00 on Sept. 30, 2008, and strong northern wind from 13:00 to 16:00 on Mar. 10, 2007.

4.1 Mean wind speed and direction

In general, the turbulence wind speed is assumed to be an ergodic process when conducting wind engineering studies. Therefore, the mean value of the whole wind sample can be replaced by the mean value of the selected sample, which is only a part of the whole wind sample. During the analysis, 10 min was taken as a basic interval, and the period when the wind speed was strongest and comparatively stable was selected. The results from analysis of the mean wind speed and direction of the five strong winds are shown in Tables 1 and 2, respectively.

The wind speeds of the four typhoons were larger than that of the strong northern wind (Table 1). Because the center of typhoon Matsa went through the RSB, the wind speed was clearly larger than that of the other typhoons. The variation in wind direction

of typhoon Fung-Wong was less than that of the other typhoons, and the direction of the strong northern wind was more stable than that of the typhoons (Table 2).

Table 1 Maximum values of the 10-min mean wind speed in samples from five strong wind events on the Runyang Suspension Bridge (m/s)

Typhoon Matsa	Typhoon Khanun	Typhoon Wipha	Typhoon Fung-Wong	Northern wind
17.86	11.13	13.43	15.36	10.91

Table 2 Variation in the 10-min mean wind direction in samples from five strong wind events on the Runyang Suspension Bridge (°)

Typhoon Matsa	Typhoon Khanun	Typhoon Wipha	Typhoon Fung-Wong	Northern wind
<50	<55	<40	<25	<25

4.2 Wind speed variation with altitude

The wind speed at 10 m (standard altitude) altitude is often taken as the basic wind speed. However, the altitude of structures such as long-span bridges is often higher than 10 m, so in bridge wind resistance design, it is necessary to convert the basic wind speed to the wind speed at any altitude.

Results show that the wind speed gradually increases with altitude from the ground to the border layer of the atmosphere, but the wind speed at different altitudes is closely related to the roughness of the ground beneath, so many kinds of expressions for the contour line of the wind speed have been proposed based on theoretical deduction and experimental studies. These expressions are of two main types, logarithmic and exponential, but all of them are generally suitable for a certain altitude (generally below 200 m). The specification assumes that the relationship between wind speed and altitude in the border layer obeys the exponent rule as follows:

$$\frac{U_2}{U_1}=\left(\frac{Z_2}{Z_1}\right)^{\alpha}, \tag{1}$$

where U_1 and U_2 are wind speeds at altitudes Z_1 and Z_2, respectively, and α is the exponent influenced by the roughness of the ground.

Two anemometers were installed in the SHMS of the RSB, one on the top of the south tower and the other in the middle of the main span (Fig. 2), so that we could obtain a set of wind speed data from each of two different altitudes. Values of α were calculated using Eq. (1) based on the two sets of wind data measurements (Table 3).

Table 3 values of α of the selected strong winds

Typhoon Matsa	Typhoon Khanun	Typhoon Wipha	Typhoon Fung-Wong	Northern wind	Specification
0.1206	0.1183	0.1209	0.1230	0.1217	0.1200

In the specification, α value corresponding to the roughness of the RSB site is 0.1200. All of α values range from 0.1150 to 0.1250, and are very close to 0.1200 (Table 3), which proves that the exponential expression suggested by the specification can suit well the wind characteristics of the RSB site. Because the height of the anemometer on the top of the south tower is 218.905 m above ground, Table 3 also shows that Eq. (1) is effective when the height is a little over 200 m.

4.3 Turbulence intensity

Turbulent flow is an extremely irregular movement, so in structural wind engineering research, it is often divided into the mean wind and the turbulence wind to simplify the analysis. As one of the key parameters reflecting the turbulence characteristic, the turbulence intensity I_i (i=u, v, w) is represented by the ratio of the mean square deviation of turbulence wind speed (σ_u, σ_v and σ_w) to the mean wind speed:

$$I_i=\frac{\sigma_i}{U},\ i=u, v, w, \tag{2}$$

where U is the mean wind speed; σ_u, σ_v and σ_w denote the average variability ranges of the turbulence wind (mean square deviation) in three directions (along-wind, across-wind and vertical direction); and I_u, I_v and I_w are the turbulence intensities in the above three directions. Therefore, according to Eq. (2), it is easy to calculate the turbulence intensity value using the wind measurement data. For comparison, the maximum and the average values of the 10-min turbulence intensity of the five strong wind events are shown in Tables 4 and 5, respectively.

Table 4 Maximum values of the 10-min turbulence intensity

Strong winds	I_u (%)	I_v (%)	I_w (%)
Typhoon Matsa	23.02	20.22	
Typhoon Khanun	39.21	31.05	
Typhoon Wipha	29.37	26.69	13.13
Typhoon Fung-Wong	24.12	24.85	12.90
Northern wind	21.68	20.04	15.36

Table 5 Average values of the 10-min turbulence intensity

Strong winds	$\overline{I_u}$ (%)	$\overline{I_v}$ (%)	$\overline{I_w}$ (%)	$\overline{I_v}/\overline{I_u}$	$\overline{I_w}/\overline{I_u}$
Typhoon Matsa	10.95	10.44		0.95	
Typhoon Khanun	21.31	20.98		0.98	
Typhoon Wipha	19.72	18.66	8.76	0.95	0.44
Typhoon Fung-Wong	11.34	11.42	6.79	1.01	0.60
Northern wind	16.02	14.22		0.89	

The anemometer in the middle of the main span is 69.300 m above ground, and the specification suggests that the along-wind turbulence intensity value at 50–70 m above ground in the open water field should be 11%. The turbulence intensity values of the typhoons Khanun and Wipha, and the strong northern wind were greater than 14% (Tables 4 and 5), mainly as a result of their relative low wind speeds.

The specification suggests that I_v should be equal to $0.88I_u$ when there are no data measurements, but Tables 4 and 5 show that I_v was greater than $0.88I_u$ and the I_v values of some typhoons were larger than the I_u. For example, both the $\overline{I_v}$ and I_v values of typhoon Fung-Wong were larger than the corresponding $\overline{I_u}$ and I_u values. In addition, the suggested value of $\overline{I_w}/\overline{I_u}$ is 0.5, while the corresponding values for typhoons Wipha and Fung-Wong were 0.44 and 0.60, respectively. Therefore, the current specification is not completely suited for the RSB in respect of turbulence intensity.

To show the variation in turbulence intensity in detail, Figs. 4–6 give all the values of turbulence intensity of some typical strong winds.

There was an obvious correlation between the along-wind and across-wind turbulence intensity values for the same strong wind (Figs. 4–6). Taking typhoon Wipha as an example, the variation in the along-wind and across-wind values during the typhoon was similar, and both of the turbulence intensity maximums appear near data point No. 60.

4.4 Turbulence integral length

Based on the data measurements, the along-wind turbulence integral length (L_u^x) and the across-wind turbulence integral length (L_v^x) were both calculated using the auto-correlation function integral method as follows (Simiu and Scanlan, 1996):

$$L_i^x = \frac{U}{\sigma_i^2}\int_0^\infty R_i(\tau)\mathrm{d}\tau,\ i=u, v, w, \qquad (3)$$

where $R_i(\tau)$ represents the auto-correlation function of the across-wind turbulence. The values of L_i^x are greatly influenced by the length and stability of the recorded data, so the measured L_i^x results of different winds differ greatly. The integral finishes when the correlation coefficient declines to less than 0.05. The maximum, average and minimum values of the 10-min turbulence integral length of each of the five strong winds are shown in Table 6.

There was no obvious relationship between the turbulence integral length and the wind speed of the strong winds, and no clear regularities were found between the typhoon and the strong northern wind with respect to turbulence integral length (Table 6). In addition, the relationship between L_u^x and L_v^x is not clear. These conclusions need to be confirmed by future wind characteristic studies.

As for the specification, the suggested values of $\overline{L_u^x}$ and $\overline{L_v^x}$ are 120 and 60 m, respectively. Table 6 shows that the $\overline{L_u^x}$ of typhoons Khanun and Wipha fit the specification well, while the $\overline{L_v^x}$ value for typhoon Fung-Wong shows the best fit. It is difficult to predict accurately the values of $\overline{L_u^x}$ and $\overline{L_v^x}$ because of the large variety of typhoons.

To obtain the correlation between the turbulence integral length and the wind speed, we examined the relationship between the maximum of the 10-min turbulence integral length and the 10-min mean wind speed (Fig. 7), and the relationship between the average of the turbulence integral length and the mean wind speed (Fig. 8).

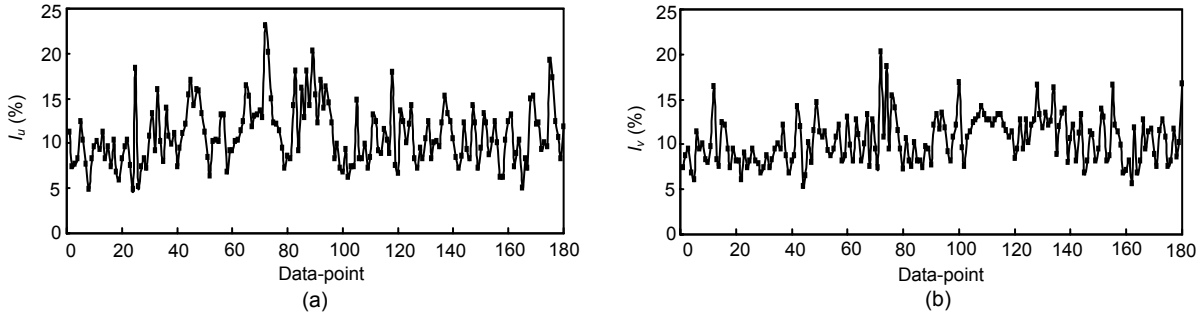

Fig. 4 10-min turbulence intensities of typhoon Matsa
(a) Along-wind; (b) Across-wind

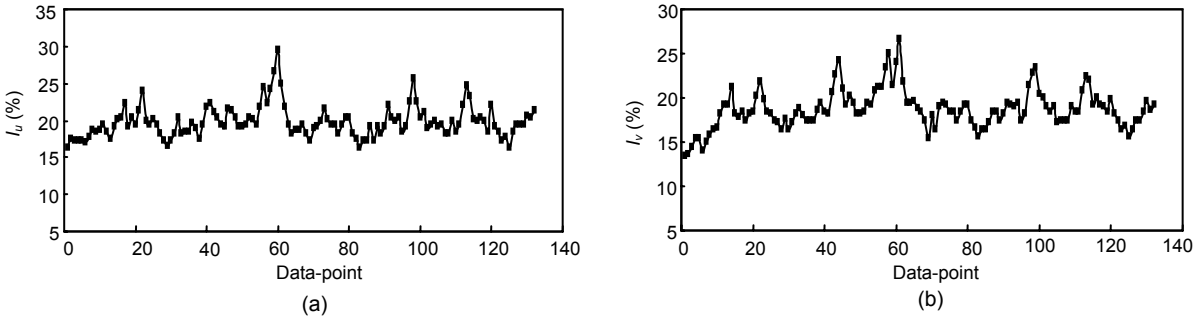

Fig. 5 10-min turbulence intensities of typhoon Wipha
(a) Along-wind; (b) Across-wind

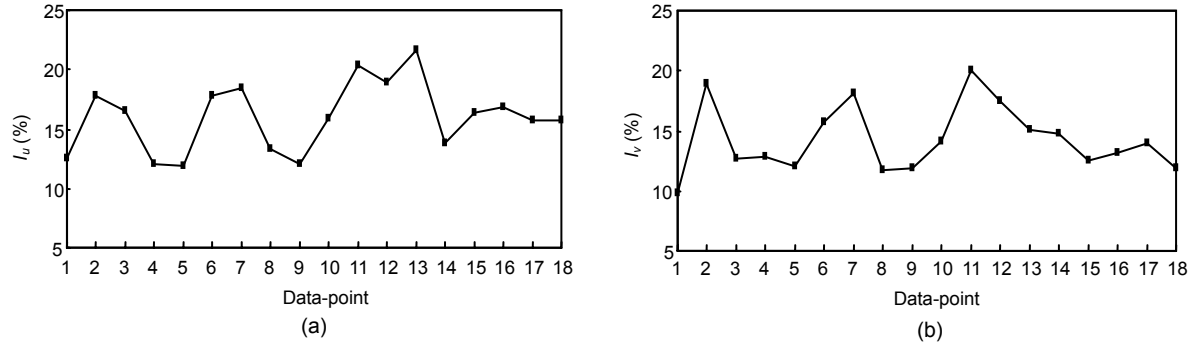

Fig. 6 10-min turbulence intensities of strong northern wind
(a) Along-wind; (b) Across-wind

To present the turbulence integral length of the typhoon characteristics of the RSB more clearly, Table 7 shows the main range in the 10-min turbulence integral length of the five strong wind events. This is also of great significance when simulating the 3D turbulence wind field.

The L_u^x ranges mainly from 50–200 m, and the L_v^x mainly from 20–100 m (Table 7). The turbulence integral lengths of the selected five strong wind events are different from one another.

4.5 Turbulence power spectrum density

As one of the key turbulence characteristics, the power spectral density can reflect the corresponding distribution of various frequencies of the turbulence and is the basis of wind field simulation. One important method for acquiring the turbulence power spectral density is to carry out the least-square fitting function based on extensive wind measurement records. Davenport (1961) simulated the along-wind turbulence wind spectrum based on more than 90 sets of strong wind data recorded in different places around the world and at different altitudes, and this was modified in later studies. The current specification for bridges adopts the Kaimal spectrum (Kaimal *et al.*, 1972). If the wind speed at Z altitude is U, then the along-wind turbulence wind power spectrum density function can be expressed as

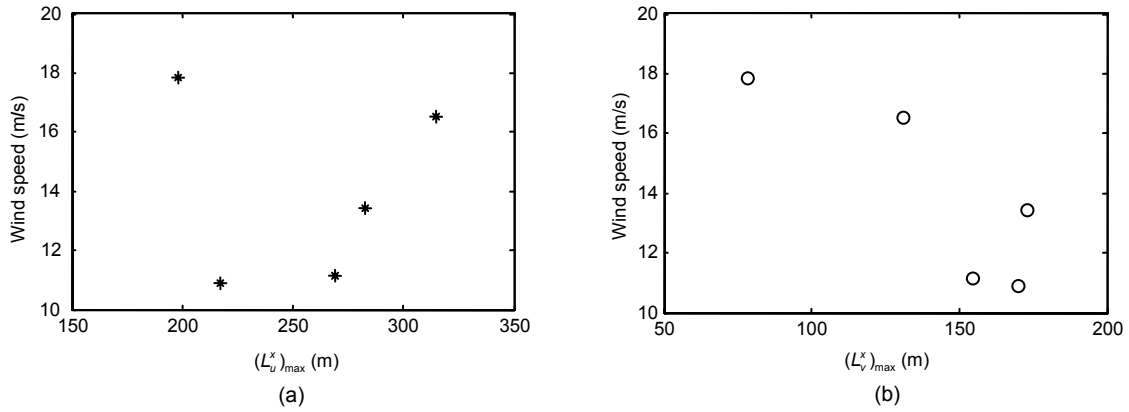

Fig. 7 Relationship between the maximum of the turbulence integral length and the wind speed

(a) $(\overline{L_u^x})_{max}$ (m); (b) $(\overline{L_v^x})_{max}$ (m)

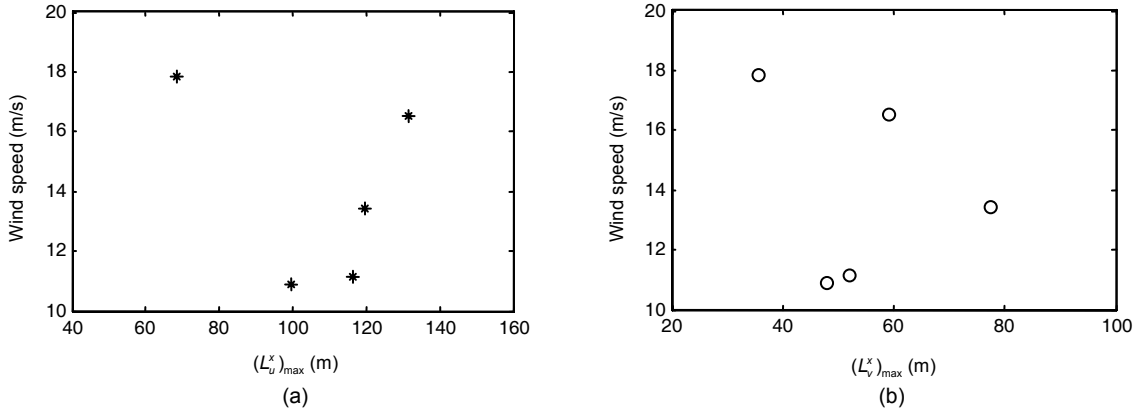

Fig. 8 Relationship between the average of the turbulence integral length and the wind speed

(a) $(\overline{L_u^x})_{max}$ (m); (b) $(\overline{L_v^x})_{max}$ (m)

Table 6 Maximum, average and minimum values of the 10-min turbulence integral length (m)

Strong winds	$(L_u^x)_{max}$	$(L_v^x)_{max}$	$\overline{L_u^x}$	$\overline{L_v^x}$	$(L_u^x)_{min}$	$(L_v^x)_{min}$
Typhoon Matsa	197.8	78.6	68.4	35.6	13.2	8.9
Typhoon Khanun	269.3	154.8	116.4	52.2	20.1	8.9
Typhoon Wipha	282.5	173.1	119.7	77.6	17.4	10.5
Typhoon Fung-Wong	314.1	129.4	132.2	58.1	17.5	10.8
Northern wind	217.3	169.9	99.6	48.1	24.7	9.7

Table 7 Range of the 10-min turbulence integral length (m)

Strong winds	$(L_u^x)_{range}$	$(L_v^x)_{range}$
Typhoon Matsa	20–160	10–80
Typhoon Khanun	70–200	20–100
Typhoon Wipha	60–180	30–130
Typhoon Fung-Wong	80–220	30–100
Northern wind	60–150	30–100

$$\frac{nS_u(n)}{(u^*)^2}=\frac{200f}{(1+50f)^{5/3}}, \tag{4}$$

$$f=nZ/U, \tag{5}$$

where S_u is the auto-power spectral density of along-wind turbulence, n is the frequency of the wind speed, Z is the height of the wind speed relative to sea

level, u^* is the wind friction speed, and f is the Moning coordinates. Because there are no data measurements of u^* in the field wind test of the RSB, the value of u^* can be calculated by the energy unitary method as (Simiu and Scanlan, 1996):

$$\sigma_u^2=6(u^*)^2. \quad (6)$$

The value of u^* has a great influence on the turbulence wind power spectrum density function, but only a few measured values of u^* have been recorded.

Considering the importance of measured values of wind friction speed, Table 8 shows the measured $(u^*)^2$ values of the five strong winds.

The measured $(u^*)^2$ values ranged from 0.5 to 1.0, and the $(u^*)^2$ value of the strong northern wind was smaller that that of the typhoons (Table 8). In addition, the $(u^*)^2$ value increased with the wind speed compared with Table 1.

During the turbulence wind power spectrum analysis, the size of fast Fourier transform (FFT) was 1024 with a frequency increment of 0.00175 Hz between two adjacent data points. The piecewise smoothing method and the Hamming window were adopted to reduce the signal leakage in the frequency domain and the piecewise smoothing technique was used to reduce the random error of spectral estimates. Fig. 9 show comparisons between the turbulence

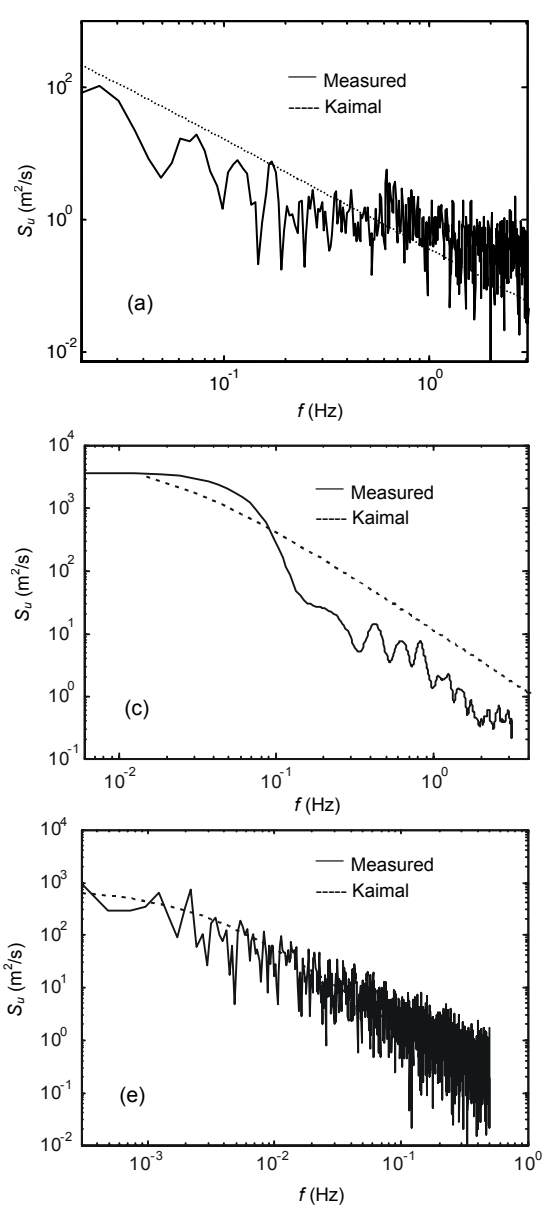

Fig. 9 Comparison of the spectra of typhoon (a) Matsa, (b) Khanun, (c) Wipha, (d) Fung-Wong, and (e) the strong northern wind and the Kaimal spectra

Table 8 Values of the wind friction speed (m^2/s^2)

Strong winds	Typhoon Matsa	Typhoon Khanun	Typhoon Wipha	Typhoon Fung-Wong	Northern wind
$(u^*)^2$	0.837	0.607	0.727	0.930	0.485

power spectrum function based on the data measurements and the Kaimal spectrum, for each of the five strong winds.

None of the five turbulence power spectrum density functions based on the measured strong winds coincide well with the Kaimal spectrum (Fig. 9). As for typhoons Matsa, Khanun, and Fung-Wong, and the strong northern wind, they are a little lower in the low frequency domain and a little higher in the high frequency domain, which shows that the horizontal turbulence kinetic energy distribution of typhoon Matsa was more concentrated in the high domain.

The turbulence power spectrum density of typhoon Wipha was a little higher in one part of the low frequency domain and a little lower in other frequency domains, which is almost converse to the cases of the other strong winds. The strong random characteristics of typhoons are further confirmed.

Relatively, the along-wind turbulence power spectrum of the strong northern wind has the closest match with the Kaimal spectrum from measured wind speed according to this study, which proves that the strong northern wind fits the specification better than the typhoons.

To study the time-variable characteristics of the along-wind turbulence power spectrum of the typhoons, the data were divided into three phases: before the typhoon, during the typhoon, and after the typhoon. A comparative analysis of the along-wind turbulence power spectrum of the three phases was conducted. Only two typical typhoons, Wipha and Fung-Wong were analyzed (Fig. 10).

The time-variable characteristics of the along-wind turbulence power spectrum of the two typhoons were similar (Fig. 10). In general, with an increase in wind speed, the along-wind turbulence power spectrum value became larger. When the wind speed decreased after the typhoon, the along-wind turbulence power spectrum value began to decline. These results provide a measurement reference for determining the wind loads of different phases when a full-course buffeting response analysis of engineering structures under typhoons is conducted.

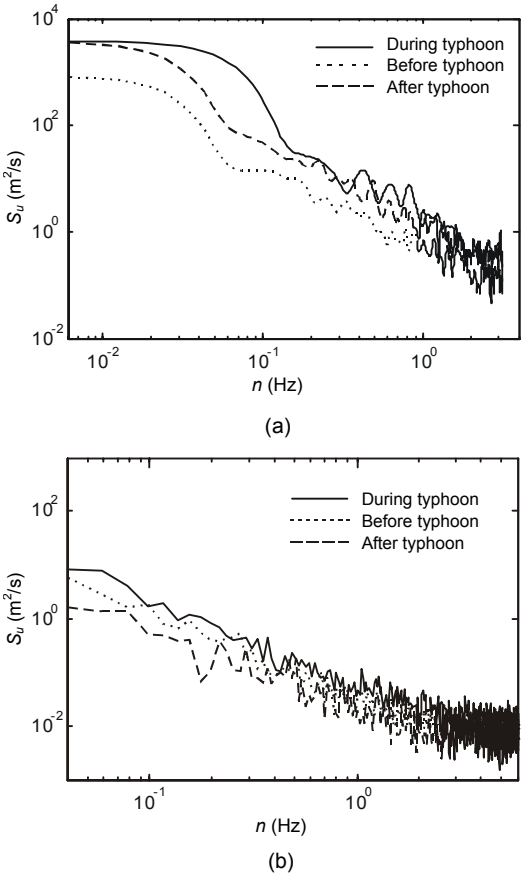

Fig. 10 Comparison of the along-wind turbulence power spectrum
(a) Typhoon Wipha; (b) Typhoon Fung-Wong

5 Conclusions

1. The wind speed of the strong northern wind is smaller than that of a typical typhoon, and the wind direction of the strong northern wind is more stable. Therefore, in summer the typhoon is the dominant wind load acting on the RSB.

2. As for the wind speed variation with altitude, the exponential expression suggested by the specification suits the wind characteristics of the RSB site very well. Moreover, Eq. (1) suggested by the specification is also effective when the height above ground is a little over 200 m.

3. Field measurement results have shown that the turbulence intensity value increases with the wind speed, and most measured values of along-wind turbulence intensity of the five selected strong winds were larger than that suggested by the specification.

In addition, the measured I_v was greater than 0.9, while the specification suggests that I_v should be equal to $0.88I_u$. Therefore, the current specification is not completely suited to the RSB with regard to turbulence intensity.

4. The L_u^x of the RSB site ranged mainly from 50–200 m, and the L_v^x ranged mainly from 20–100 m. There was no obvious relationship between the turbulence integral length and the wind speed, and no clear regularities could be found between the typhoon and the strong northern wind in respect of turbulence integral length. In addition, the relationship between L_u^x and L_v^x was unclear.

5. The measured $(u^*)^2$ values of the five strong winds of the the RSB site ranged mainly from 0.5 to 1.0, and the $(u^*)^2$ value of the strong northern wind was relatively small than those of the typhoons. In addition, the $(u^*)^2$ values increased with the wind speed in general.

6. The along-wind turbulence power spectrum density functions of the measured strong winds did not coincide well with the Kaimal spectrum. Relatively, the spectrum of the strong northern wind matched the Kaimal spectrum better than that of the typhoon. As for the typhoon, the along-wind turbulence power spectrum value became larger with increasing wind speed.

References

Andersen, O.J., Lovseth, J., 1995. Gale force maritime wind, the Froya data base. Part 1: sites and instrumentation, review of the database. *Journal of Wind Engineering and Industrial Aerodynamics*, **57**(1):97-109. [doi:10.1016/0167-6105(94)00101-I]

Chen, Z.Q., Wang, X.Y., Ko, J.M., Ni, Y.Q., 2002. Field measurements on wind-rain-induced vibration of bridge cables with and without MR dampers. The 3rd World Conference on Structural Control, Como, Italy.

Choi, E.C.C., 1978. Characteristics of typhoons over the southeast China sea. *Journal of Wind Engineering and Industrial Aerodynamics*, **3**(4):353-365. [doi:10.1016/0167-6105(78)90038-7]

Davenport, A.G., 1961. The spectrum of horizontal gustiness near the ground in high winds. *Quarterly Journal of the Royal Meteorological Society*, **87**(372):194-211. [doi:10.1002/qj.49708737208]

Davenport, A.G., 1962. Buffeting of a suspension bridge by storm winds. *Journal of Structural Division, ASCE*, **88**(ST3):233-268.

Ge, Y.J., Xiang, H.F., 2004. Recent Development of Bridge Aerodynamics in China. The 5th International Colloquium on Bluff Body Aerodynamics and Applications, Ottawa, Canada. [doi:10.1016/j.jweia.2007.06.045]

Geurts, C.P.W., Rutten, H.S., Wisse, J.A., 1996. Coherence of wind-induced pressures on buildings in urban areas: set up of a full-scale experiment. *Journal of Wind Engineering and Industrial Aerodynamics*, **65**(1-3):31-41. [doi:10.1016/S0167-6105(97)00020-2]

Holmes, J.D., 2001. Wind Loading of Structures. Spon Press, London.

Hui, M.C., Larsen, A., Xiang, H.F., 2009. Wind turbulence characteristics study at the Stonecutters Bridge site: Part I —Mean wind and turbulence intensities. *Journal of Wind Engineering and Industrial Aerodynamics*, **97**(1):22-36. [doi:10.1016/j.jweia.2008.11.002]

Kaimal, J.C., Wyngaard, J.C., Izumi, Y., Cote, O.R., 1972. Spectral characteristics of surface-layer turbulence. *Quarterly Journal of the Royal Meteorological Society*, **98**(417):563-589. [doi:10.1002/qj.49709841707]

Kato, N., Ohukuma, T., Kim, J.R., Marukawa, H., Niihori, Y., 1992. Full scale measurements of wind velocity in two urban areas using an ultrasonic anemometer. *Journal of Wind Engineering and Industrial Aerodynamics*, **41-44**(1-3):67-78. [doi:10.1016/0167-6105(92)90394-P]

Law, S.S., Bu, J.Q., Zhu, X.Q., 2006. Wind characteristics of Typhoon Dujuan as measured at a 50 m guyed mast. *Wind and Structure*, **9**(5):387-396.

Li, Q.S., Wu, J.R., Liang, S.G., Xiao, Y.Q., Wong, C.K., 2004. Full-scale measurements and numerical evaluation of wind-induced vibration of a 63-story reinforced concrete super tall building. *Engineering Structures*, **26**(12):1779-1794. [doi:10.1016/j.engstruct.2004.06.014]

Miyata, T., Yamada, H., Katsuchi, H., Kitagawa, M., 2002. Full-scale measurements of Akashi-Kaikyo Bridge during typhoon. *Journal of Wind Engineering and Industrial Aerodynamics*, **90**(12-15):1517-1527. [doi:10.1016/S0167-6105(02)00267-2]

Naito, G., 1988. Turbulent proper ties and spectral behaviors of ocean winds observed at an offshore tower. *Journal of Wind Engineering and Industrial Aerodynamics*, **28**(1-3):51-60.

Pang, J.B., Lin, Z.X., Ge, Y.J., 2002. Field measurements of strong wind characteristics in Pudong district. *Experiments and Measurements in Fluid Mechanics*, **16**(3):32-39 (in Chinese).

Panofsky, H.A., Dutton, J.A., 1984. Atmospheric Turbulence-models and Methods for Engineering Application. John Wiley & Sons, Inc, New York.

Rigato, A., Chang, P., Simiu, E., 2001. Database-assisted design, standardization and wind direction effects. *Journal of Structural Engineering*, **127**(8):855-860. [doi:10.1061/(ASCE)0733-9445(2001)127:8(855)]

Shiau, B.S., Chen, Y.B., 2001. Measurement study on the typhoon Bilis—wind velocity spectrum and turbulence characteristics near the ground. *Atmospheric Research*, **57**(3):171-185. [doi:10.1016/S0169-8095(01)00069-2]

Simiu, E., Scanlan, R.H., 1996. Wind Effects on Structures. John Wiley & Sons, Inc, New York.

Siringoringo, D.M., Fujino, Y., 2008. System identification of suspension bridge from ambient vibration response. *Engineering Structures*, **30**(2):462-477. [doi:10.1016/j.engstruct.2007.03.004]

Sparks, P.R., Reid, G.T., Reid, W.D., Welsh, S., Welsh, N., 1992. Wind conditions in hurricane Hugo by measurement, inference, and experience. *Journal of Wind Engineering and Industrial Aerodynamics*, **41**(1-3):55-66. [doi:10.1016/0167-6105(92)90393-O]

Tieleman, H.W., 2008. Strong wind observations in the atmospheric surface layer. *Journal of Wind Engineering and Industrial Aerodynamics*, **96**(1):41-77. [doi:10.1016/j.jweia.2007.03.003]

Vickery, P.J., Twisdale, L.A., 1995. Wind-field and filling models for hurricane wind-speed predictions. *Journal of Structural Engineering*, **121**(11):1700-1709. [doi:10.1061/(ASCE)0733-9445(1995)121:11(1700)]

Wang, H., Li, A.Q., Xie, Y.S., 2009. Field measurement on wind characteristic and buffeting response of the Runyang Suspension Bridge during typhoon Matsa. *Science China Technological Sciences*, **52**(5):1354-1362. [doi:10.1007/s11431-008-0238-y]

Xiang, H.F., 2004. Wind-resistant Design Specification for Highway Bridges. China Communications Press, Beijing (in Chinese).

Xu, Y.L., Zhu, L.D., 2005. Buffeting response of long-span cable-supported bridges under skew winds: case study. *Journal of Sound and Vibration*, **281**(3-5):675-687. [doi:10.1016/j.jsv.2004.01.025]

Xu, Y.L., Zhu, L.D., Wong, K.Y., 2000. Field measurement results of Tsing Ma Suspension Bridge during Typhoon Victor. *Structure Engineering and Mechanics*, **10**(6):545-559.

2009 JCR of Thomson Reuters for *JZUS-A*

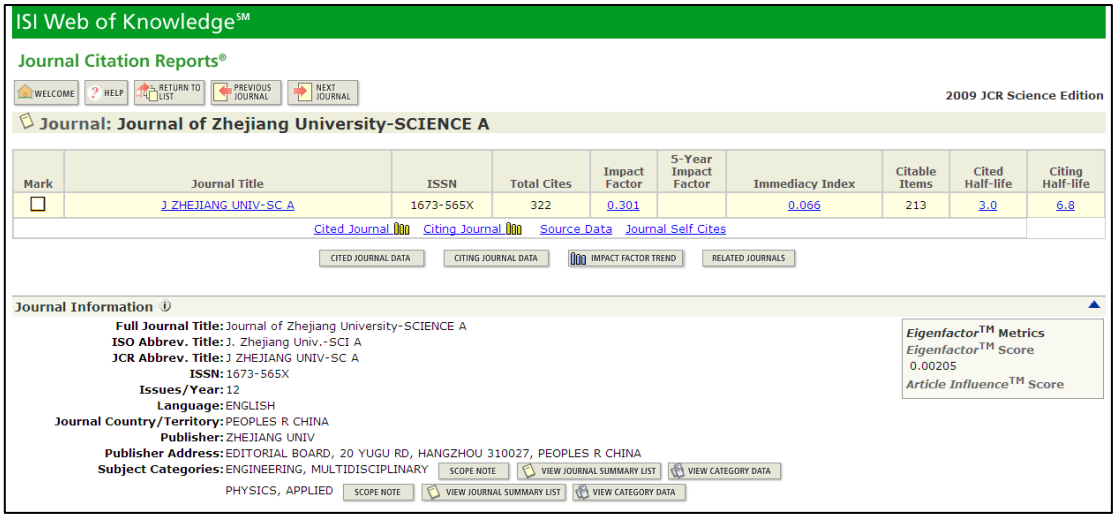

ISI Web of Knowledge℠

Journal Citation Reports®

WELCOME | HELP | RETURN TO LIST | PREVIOUS JOURNAL | NEXT JOURNAL

2009 JCR Science Edition

Journal: Journal of Zhejiang University-SCIENCE A

Mark	Journal Title	ISSN	Total Cites	Impact Factor	5-Year Impact Factor	Immediacy Index	Citable Items	Cited Half-life	Citing Half-life
☐	J ZHEJIANG UNIV-SC A	1673-565X	322	0.301		0.066	213	3.0	6.8

Cited Journal | Citing Journal | Source Data | Journal Self Cites

CITED JOURNAL DATA | CITING JOURNAL DATA | IMPACT FACTOR TREND | RELATED JOURNALS

Journal Information

Full Journal Title: Journal of Zhejiang University-SCIENCE A
ISO Abbrev. Title: J. Zhejiang Univ.-SCI A
JCR Abbrev. Title: J ZHEJIANG UNIV-SC A
ISSN: 1673-565X
Issues/Year: 12
Language: ENGLISH
Journal Country/Territory: PEOPLES R CHINA
Publisher: ZHEJIANG UNIV
Publisher Address: EDITORIAL BOARD, 20 YUGU RD, HANGZHOU 310027, PEOPLES R CHINA
Subject Categories: ENGINEERING, MULTIDISCIPLINARY | SCOPE NOTE | VIEW JOURNAL SUMMARY LIST | VIEW CATEGORY DATA
PHYSICS, APPLIED | SCOPE NOTE | VIEW JOURNAL SUMMARY LIST | VIEW CATEGORY DATA

Eigenfactor™ Metrics
Eigenfactor™ Score
0.00205
Article Influence™ Score